

Photo-induced spin and valley-dependent Seebeck effect in the low-buckled Dirac materials

Yawar Mohammadi *

Department of physics, Farhangian University, Tehran, Iran

Abstract

Employing the Landauer-Buttiker formula we investigate the spin and valley dependence of Seebeck effect in low-buckled Dirac materials (LBDMs), whose band structure are modulated by local application of a gate voltage and off-resonant circularly polarized light. We calculate the charge, spin and valley Seebeck coefficients of an irradiated LBDM as functions of electronic doping, light intensity and the amount of the electric field in the linear regime. Our calculation reveal that all Seebeck coefficients always shows an odd features with respect to the chemical potential. Moreover, we show that, due to the strong spin-orbit coupling in the LBDMs, the induced thermovoltage in the irradiated LBDMs is spin polarized, and can also become valley polarized if the gate voltage is applied too. It is also found that the valley (spin) polarization of the induced thermovoltage could

*Corresponding author's E-mail address: y.mohammadi@cfu.ac.ir

be inverted by reversing the circular polarization of light or reversing the direction the electric field (only by reversing the circular polarization of light).

Keywords: A. Low-buckled Dirac materials; D. Ballistic transport; D. spin/valley dependent Seebeck effect; D. off-resonant light irradiation.

1 Introduction

The low-buckled Dirac materials are monolayer honeycomb lattice structures of heavy IV-group elements. Such lattice structures have been synthesized recently for silicon[1, 2, 3, 4, 5, 6], germanium[7, 8], and also stannum[9]. They are also known as silicene, germanene and stanene respectively. In these structures, atoms arranged in a monolayer honeycomb lattice which can be described as in graphene in terms of two triangular sublattices. However, larger ionic size of heavy IV-group atoms results in buckling of these two-dimensional lattices. Accordingly, the sites on the two sublattices are shifted vertically with respect to each other and sit in two parallel planes with a separation of 0.46 nm . Due to the puckered structure, which results in a large spin-orbit interaction[10, 11], the low energy dynamic in the LBDMs is dominated by a massive Dirac Hamiltonian[10], with a mass which could also be tuned via an electric field applied perpendicular to its plane[12]. These novel features donate many attractive properties such as quantum spin Hall effect[10, 13], valley-polarized quantum Hall effect[14, 15, 16], quantum thermal transport[17], topological superconducting effect[18] and so on [19, 20, 21, 22, 23, 24, 25, 26, 27] to the LBDMs.

In the LBDMs, the valley and spin degrees of freedom have been coupled via a spin-orbit interaction[10] which is large compared with that in graphene[28]. Further, they have long spin-

coherence length[29] and spin-diffusion time[30, 31], and also weak inter-valley coupling[32]. These properties make them suitable materials to detect spin- or/and valley-dependent transport phenomena. Provided that the spin or/and valley degeneracy of their band structure are lifted[19, 33]. This can be achieved, for example, in a ferromagnetic LBDM, in which the magnetic exchange field is supposed to be induced in the LBDM, as in graphene by an adjacent magnetic insulator such as *EuO*[34], *EuS*[35] or *YIG*[36]. Based on this fact, recently various spin- and valley dependent thermoelectric effects, such as spin-valley diode effect[37], spin-valley Seebeck effect[38] and anomalous thermospin effect[39], have been predicted for the ferromagnetic LBDMs. Unfortunately, these effects can be observed *only for temperature regime lower than magnetic exchange field(h), namely for $T < h/k_B$* . In this letter we propose a new scheme to achieve the spin- and valley-dependent Seebeck effects in the LBDMs, which can also overcome the above mentioned problem of the ferromagnetic LBDMs. Our scheme is based on a new experimental technique[40, 41] which makes it possible to access effects arising from off-resonant light irradiation. In the off-resonant regime, light does not directly excite the electrons, and instead effectively modifies the electron band structure through virtual photon absorption/emission processes. Further, it has been shown that the influence of such off-resonant light is captured in a valley-dependent static effective Hamiltonian[20, 42, 43, 44]. This valley-dependent effect, due to the strong spin-valley coupling in the LBDMs, removes the spin degeneracy of their band structure and provides a new platform to explore detectable spin- and valley-dependent transport phenomena in these materials.

In this letter, employing the Landauer–Büttiker formalism we investigate the spin and valley dependence of thermoelectric effects in an irradiated LBDM-based junction exposed to a temperature gradient. Our results show that when the central region of the junction is exposed

to off-resonant circularly polarized light, the energy bands in the central region become only spin-polarized. This can lead to spin-dependent Seebeck effect, whose amount and polarization can be controlled by tuning the light intensity and circulation respectively. If a perpendicular electric field is applied too, the band structure becomes spin and valley-polarized. Consequently, the induced Seebeck effect become spin- and valley-dependent. The valley (spin) polarization of the induced Seebeck effect can be inverted by reversing the the circular polarization of light or reversing the direction of the electric field (only by reversing the the circular polarization of light). The corresponding Hamiltonian model and formalism are introduced in sec. II. We present our numerical results and discussion in sec. III and end the paper by summary and conclusions in sec. IV.

2 Model Hamiltonian

The low energy physics in a low-buckled Dirac material, which is subjected to a perpendicular electric field, is governed by a 2×2 Hamiltonian matrix as[10, 11, 12]

$$H^{\eta,s} = \hbar v_F(k_x \tau_x - \eta k_y \tau_y) - \eta s \lambda_{so} \tau_z + \lambda_z \tau_z, \quad (1)$$

acting in the sublattice pseudospin space. The first term is the Dirac Hamiltonian arising from the nearest neighbor transfer energy in a two-dimensional honeycomb lattice where $\eta = +(-)$ refers to $\mathbf{K}(\mathbf{K}')$ Dirac points and $v_F = \sqrt{3}\gamma a/2\hbar$ is the Fermi velocity with t and a being the nearest neighbor transfer energy and the lattice constant which have been listed in table 1 for silicene, germanene and stanene. Here $\mathbf{k} = (k_x, k_y)$ is the two dimensional momentum measured from Dirac points and $\tau_i (i = x, y, z)$ are Pauli matrixes. The second term is the Kane-Mele term for the intrinsic spin-orbit coupling, in which $\lambda_{so} = \lambda_{so1} + \lambda_{so2}$ with λ_{so1} and λ_{so2} being the

first and second order effective spin-orbit interaction in a low-buckled Dirac material(see table 1). In this term $s = +(-)$ index denotes to the spin-up (-down) degree of freedom. The last term is the on-site potential difference between A and B sublattices tuned by the perpendicular electric field, E_z , in which $\lambda_z = \pm edE_z$, e is the electron charge, d is the vertical distance between A and B sublattices, and $+(-)$ is used when E_z is along $+z$ ($-z$) direction.

As mentioned above, the sample is subjected to off-resonant circularly polarized light, whose vector potential can be written as $\mathbf{A}(t) = (\pm A \sin \Omega t, A \cos \Omega t)$ where Ω is the frequency of light and the plus (minus) sign denotes to the right (left) circulation. In the off-resonant regime, satisfied when $\hbar\Omega \gg \gamma$, light does not directly excite the electrons, and instead effectively modifies the electron band structure through virtual photon absorption/emission processes (see Ref. [42]). Moreover, when the intensity of light is small ($\mathcal{A} = eaA/\hbar \ll 1$), the influence of the off-resonant light irradiation on the electron band structure (According to the Floquet theory and the Peierls substitution) is well captured by a static effective Hamiltonian[20, 42, 43, 44] as $\Delta H^{\eta,s} = \eta\lambda_\Omega\tau_z$, where $\lambda_\Omega = \pm(\hbar v_F \mathcal{A}/a)^2/\hbar\Omega$ with $+(-)$ for the right (left) circulation of light. Hence, the low energy physics in low buckled honeycomb structures subjected to a perpendicular electric field and off-resonant circularly polarized light is described by an effective Hamiltonian as

$$H_{eff}^{\eta,s} = \hbar v_F(k_x\tau_x - \eta k_y\tau_y) - \eta s\lambda_{so}\tau_z + \lambda_z\tau_z + \eta\lambda_\Omega\tau_z, \quad (2)$$

acting in the sublattice pseudospin space, whose energy bands are

$$\varepsilon_s^\eta = \nu\sqrt{(\hbar v_F|\mathbf{k}|)^2 + \Delta^2}, \quad (3)$$

where $\Delta = \eta(s_z\lambda_{so} - \lambda_\Omega) - \lambda_z$ [20] and $\nu = +(-)$ denotes to the conduction (valance) band.

The low energy bands in each region of the junction (the leads and the conducting region) are

obtained from Eq. 3, just by inserting the corresponding λ_z and λ_Ω .

In this letter we study ballistic thermal transport of massive Dirac fermions through a LBDM-based junction subjected to a gradient temperature (see Figs. 1 and 5). The central region is subjected to off-resonant circularly polarized light and an electric field applied perpendicular to its plane. We take x-axis perpendicular to the interfaces and y-axis along them (see fig. 1). The interfaces of the leads and the central region are located at $x = 0$ and $x = L$. We also assume the translational invariance along y-axis satisfied in the limit of large W (W is the width of the LBDM plane). We restrict our consideration to $W/L \gg 1$ limit, in which the effects of the microscopic details of the upper and lower edges of the junction on the electron transport become insignificant [45]. According to the generalized Landauer–Büttiker approach [46], the spin and valley-resolved current driven by temperature difference, $\Delta T = T_L - T_R$, can be expressed as

$$I_{\eta,s} = \frac{e}{h} \int_{-\infty}^{\infty} [n_F(E, T_L) - n_F(E, T_R)] N(E) T_{\eta,s}(E) dE, \quad (4)$$

in which $N(E) = \frac{W\sqrt{E^2 - \lambda_{so}^2}}{\sqrt{3\pi}ta}$ is the density of states at the leads, $n_F(E, T_{L(R)}) = \frac{1}{[e^{(E - \mu_{L(R)})/k_B T_{L(R)}} + 1]}$ is the Fermi-Dirac distribution function of the carriers at left(right) lead, and $T_{\eta,s}(E)$ can be written in terms of the valley/spin dependent transmission coefficient as

$$T_{\eta,s}(E) = \int_{-\pi/2}^{+\pi/2} |t_\eta^s(E, \phi)|^2 d\phi, \quad (5)$$

where $\phi = \tan^{-1}(k_y/k_x)$ is the angle of incidence and $t_{\eta,s}(E, \phi)$ represents the transmission coefficient obtained by matching the wave functions and their derivatives at the interfaces. The wave functions for the valley η and the spin s in the left and right lead can be written

respectively as

$$\psi_{\nu,L}^{\eta,s} = e^{ik_y y} \left[\frac{e^{ik_x x}}{\sqrt{2\chi_L}} \begin{pmatrix} \sqrt{\chi_L - \nu(\eta s_z \lambda_{so})} \\ \nu e^{-i\eta\phi} \sqrt{\chi_L + \nu(\eta s_z \lambda_{so})} \end{pmatrix} + r_{\eta,s} \frac{e^{-ik_x x}}{\sqrt{2\chi_L}} \begin{pmatrix} \sqrt{\chi_L - \nu(\eta s_z \lambda_{so})} \\ \nu e^{-i\eta(\pi-\phi)} \sqrt{\chi_L + \nu(\eta s_z \lambda_{so})} \end{pmatrix} \right], \quad (6)$$

and

$$\psi_{\nu,R}^{\eta,s_z} = t_{\eta,s} \frac{e^{i(k_x x + k_y y)}}{\sqrt{2\chi_L}} \begin{pmatrix} \sqrt{\chi_L - \nu(\eta s_z \lambda_{so})} \\ \nu e^{-i\eta\phi} \sqrt{\chi_L + \nu(\eta s_z \lambda_{so})} \end{pmatrix}, \quad (7)$$

respectively, where $\chi_L = \sqrt{(\hbar v_F k)^2 + \lambda_{so}^2}$, $r_{\eta,s}$ is the reflection coefficient and $\nu = +(-)$ denotes to the conduction (valance) band. The corresponding wave function in the conduction region is given by

$$\psi_{\nu,C}^{\eta,s} = e^{iq_y y} \left[a_{\eta,s_z} e^{iq_x x} \begin{pmatrix} \sqrt{\chi_C - \nu\Delta} \\ \nu e^{-i\eta\theta} \sqrt{\chi_C + \nu\Delta} \end{pmatrix} + b_{\eta,s} e^{-iq_x x} \begin{pmatrix} \sqrt{\chi_C - \nu\Delta} \\ \nu e^{-i\eta(\pi-\theta)} \sqrt{\chi_C + \nu\Delta} \end{pmatrix} \right], \quad (8)$$

where $\chi_C = \sqrt{(\hbar v_F q)^2 + \Delta^2}$ and $\theta = \tan^{-1}(q_y/q_x)$ is the refractive angle at the interface. We restrict our calculations to the elastic scattering at the interfaces, which yields $k \sin \phi = q \sin \theta$, with $k = (\hbar v_F)^{-1} \sqrt{E^2 - \lambda_{so}^2}$ and $q = (\hbar v_F)^{-1} \sqrt{E^2 - \Delta^2}$. The coefficients a_{η,s_z} and b_{η,s_z} could be determined by requiring continuity of the wave functions. Matching the wave functions at the interfaces yields

$$t_{\eta,s_z} = (\cos(q_x L) - i\mathcal{F}(E, \phi) \sin(q_x L))^{-1}, \quad (9)$$

for the transmission coefficient in which

$$\mathcal{F}(E, \phi) = \frac{k_x^2 \varepsilon_C^2 + q_x^2 \varepsilon_L^2 + k_y^2 (\varepsilon_C - \varepsilon_L)^2}{2\varepsilon_L \varepsilon_C k_x q_x}, \quad (10)$$

where $\varepsilon_L = |E| + \lambda_{so}$ and $\varepsilon_C = |E| + |\Delta|$.

Employing the linear response assumption[47], i.e., $T_L \approx T_R = T$, we obtain from Eq. 4 the spin- and valley-resolved thermopower as

$$S_{\eta,s_z} = -\frac{1}{eT} \frac{L_{\eta,s}^1}{L_{\eta,s}^0}, \quad (11)$$

with $L_{\eta,s}^{n(=0,1)} = \frac{1}{\hbar} \int dE (E - \mu)^n \int d\alpha \cos \alpha T_{\eta,s}(E) [-\partial_E f(E)]$. In analogy with the charge thermopower, $S_c = \sum_{\eta,s} S_{\eta,s_z}/2$, one can define the spin- and valley-dependent thermopower, calculated as [48] $S_s = \sum_{\eta,s} s S_{\eta,s_z}$ and $S_v = \sum_{\eta,s} \eta S_{\eta,s_z}$ respectively. The spin- and/or valley-dependent Seebeck effect is observed when S_s and/or S_v become nonzero. The corresponding numerical results are presented in the next section.

3 Results and Discussion

In this section we present our numerical results for the photo-induced spin- and valley-dependent Seebeck effect in the LBDM-based junctions. This will be done by calculating the charge, spin and valley Seebeck coefficients (S_c , S_s and S_v) for an irradiated LBDM-based junction. We present our results in two cases. In the first one, the central region of the LBDM-junction is subjected only to off-resonant circularly polarized light, but in the second one it is simultaneously exposed to off-resonant circularly polarized light and a vertical electric field.

First we explain the general features of the Seebeck effect in the LBDM-based junctions. The LBDMs are semiconductors with small band gaps. So temperature can play the role of exciting thermo-electrons in the LBDMs, and both electrons and holes can contribute to their transport phenomena even in the undoped regime. Additionally, according to Eq. 11, to induce Seebeck effect in a LBDM, the number of the transmission modes must be asymmetric about the Fermi energy. In our scheme, this is satisfied only when LBDM becomes electron- or hole-

doped, which can be done by a back gate voltage[49] or by depositing alkali metals on the surface[50] as in graphene. In the doped regime the thermally activated electrons (hole), which move in the direction (the opposite direction) of the temperature gradient (see Eq. 4), result in different charge accumulations at both sides of the junction, namely $S_c \neq 0$. So, depending on whether the LBDM-based junction is electron or hole doped, the charge thermopower becomes positive or negative. This can be seen in the panel (a) of Fig. 2 (the black curve), in which we exhibit the charge thermopower of a LBDM-based junction as a function of *scaled chemical potential*, μ/λ_{so} . Furthermore, the charge thermopower shows an odd feature respect to the chemical potential, namely $S_c(-\mu) = -S_c(\mu)$. This is similar to the well-known effect in semiconductors in which the thermopower for n and p-type ones has opposite sign. However, in a LBDM-based junction the sign of the thermopower can be changed easily by tuning the chemical potential. Moreover, one can see that, in the absence of off-resonant light irradiation ($\lambda_\Omega = 0$), the induced Seebeck effect is not spin polarized (see the black curve of Fig. 3(b)). This is due to the spin degeneracy of the band structure of the LBDMs, which leads to same accumulation for both spin-up and spin-down charge carriers at both sides of the junction. Note, although the spin degeneracy in each valley can be lifted via a vertical electric field, this can not induce spin-dependent transport effect[22].

In our proposed method, to achieve spin-dependent Seebeck effect, the central region of the LBDM-based junction is irradiated by off-resonant circularly polarized light (see Fig. 1). Consequently, as discussed above, light modifies the energy bands through virtual photon absorption/emission processes, making them spin polarized with same polarization at \mathbf{K} and \mathbf{K}' valley (see panel (c) and (d) of Fig. 1). This can lead to a spin-dependent Seebeck effect as shown in the panel (b) of Fig. 1, in which the spin thermopower of a LBDM-based junction

have been drawn as a function of the scaled chemical potential for different λ_Ω at temperature $T = 0.4\lambda_{so}/k_B$. It is evident that the spin thermopower, like the charge thermopower, shows an odd feature respect to the chemical potential. However, the charge and the spin thermopower have opposite sign at same chemical potential. Moreover, one can see that both the spin and charge thermopowers can be enhanced by increasing the light intensity (increasing λ_Ω).

Figure 3 shows the charge and spin thermopower of an irradiated LBDM-based junction as a function of the scaled chemical potential for different temperatures. It is evident that the amounts of S_c and S_s decrease by increase of temperature. This can be explained as follows; At low temperatures the energy broadening of the derivative of Fermi-Dirac distribution function, that determines which electrons or holes could contribute to the Seebeck effect, is small. So, for $\mu > 0$ ($\mu < 0$) the Seebeck effect is mostly induced by thermally activated electrons (holes) with special spin index. By increasing the temperature of the junction, the the energy broadening of $\partial_E f(E)$ increases and it overlaps with the other energy bands, which results in S_c and/or S_s with opposite sign. Hence, the induced spin and charge thermovoltage decreases. Moreover, one can see that even at high temperatures, at which the exchange interaction induced in the ferromagnetic LBDM-based junctions will be quenched, the amount of the spin thermopower of the irradiated LBDM-based junction is large. Based on numerical results, it is about $0.15mV/K$ at 36K, 430K and 600K for silicene, germanene and stanene respectively, which could be detected easily (see Fig. 4 (b)). *This is an important advantage of irradiated LBDM-based junctions over the ferromagnetic LBDM-based ones.*

Another important advantage of irradiated LBDM-based junctions over ferromagnetic LBDM-based ones is that *the induced spin-polarized thermovoltage in the LBDM-based junctions could be inverted easily by reversing the circular polarization of light (determined by the sign of λ_Ω).*

This can be understood based on the effect of the off-resonant light irradiation on their band structure (see the (c) and (d) panels of Fig. 1); Changing the circular polarization of light, from right to left polarization or vice versa, interchanges the spin-up and spin-down electron bands in the central region. Consequently, the spin polarization of the induced thermovoltage becomes inverted. This can be seen in the Fig. 4, in which we exhibit the charge and spin thermopower of a LBDM-based junction as a function of λ_Ω . Moreover, this figure show that the charge thermopower is an even function of the λ_Ω . This is due to this fact that changing the circulation of light just interchanges the spin-up and spin-down energy bands.

To achieve both the spin- and valley-dependent Seebeck effects at the same time, the central region of the LBDM-based junction must be simultaneously subjected to off-resonant circularly polarized light and a vertical electric filed. Hence, the band structure of the central region is modified through virtual photon absorption/emission processes and also by the vertical electric field. This leads to a new energy band which, due to the strong spin-valley coupling in the LBDMs, is spin- and valley polarized. See Fig. 5. This can lead to spin- and valley-dependent Seebeck effects. The valley (spin) polarization of the induced thermovoltage could be inverted by reversing the circular polarization of light or the direction the electric field (only by reversing the circular polarization of light). Because changing the circular polarization of light or the direction of the electric field (only changing the circular polarization of light), invert the valley (spin) polarization of the energy bands in the central region of the junction (Fig. 5 (b)-(e)).

Figures 6 and 7 show the charge and spin thermopower of the irradiated LBDM-based junction exposed to the vertical electric filed as functions of $\lambda_\Omega/\lambda_{so}$ and λ_z/λ_{so} . In the results presented in the panel (a) and (b) the chemical potential is $-0.5\lambda_{so}$ and $+0.5\lambda_{so}$ respectively. These figures, in addition to confirming our previous results *i.e.* $S_{c(s)}(-\mu) = -S_{c(s)}(\mu)$,

$S_c(-\lambda_\Omega) = S_c(\lambda_\Omega)$ and $S_s(-\lambda_\Omega) = -S_s(\lambda_\Omega)$, show that S_c and S_s are even in λ_z , namely reversing the direction of the electric field doesn't change the spin polarization of the induced thermovoltage. This can be understood based on the effect of the vertical electric field on the band structure of the junction (see Fig 5 (b)-(e)).

In Fig. 8 we have exhibited the same plots as in Figs. 6 and 7 but for the valley thermopower. Figure 8 shows that: Firstly, when both the electric field and the light irradiation are present ($\lambda_\Omega \neq 0$ and $\lambda_z \neq 0$) the induced Seebeck effect become valley dependent too, namely $S_v \neq 0$. Secondly, by only applying a vertical electric field the Seebeck effect doesn't occur. Thirdly, like S_c and S_s , the valley thermopower shows an odd feature respect to the chemical potential. *Fourthly, one can invert the valley polarization of the induced thermovoltage by reversing the circular polarization of light or reversing the direction of the electric field, $S_v(-\lambda_\Omega) = -S_v(\lambda_\Omega)$ and $S_v(-\lambda_z) = -S_v(\lambda_z)$.*

At the end a point is worth of mentioning. Our calculations (don't presented here) reveal that the plots of Seebeck coefficients of silicene, germanene and stanene, except for a minor difference at the amount of them for silicene, are equal and show same features. So, we presented our numerical results, in general, for a LBDM-based junction, and we didn't exhibit the plots for each of them separately.

4 Summary and conclusions

In summary we studied the spin and valley dependence of Seebeck effect in a LBDM-based junction, whose energy bands was assumed to be modulated by local application of a gate voltage and off-resonant circularly polarized light. Employing the Landauer-Buttiker formula we

calculated the charge, spin and valley Seebeck coefficients in the linear regime. Our calculation revealed that when the junction is only subjected to the light beam, the induced Seebeck effect is spin polarized. We showed that the spin polarization of the induced thermovoltage could be controlled by tuning the light intensity and its circulation. Moreover we found if off-resonant circularly polarized light and the vertical electric field are applied simultaneously, the induced Seebeck effect becomes valley polarized too. It was also shown that the valley (spin) polarization of the induced thermovoltage could be inverted by reversing the circular polarization of light or the direction the electric field (only by reversing the circular polarization of light). The proposed thermoelectric device has two important advantages over the ferromagnetic one. The first is that it can operate at high temperatures at which the exchange interaction induced in the ferromagnetic LBDM-based junctions will be quenched. Another important advantage is that the induced spin and valley polarized thermovoltages in the irradiated LBDM-based junctions could be inverted easily by reversing the circular polarization of light or reversing the direction of the applied electric field.

5 acknowledgment

This work was supported by farhangian university.

References

- [1] B. Lalmi, H. Oughaddou, H. Enriquez, A. Kara, S. Vizzini, B. Ealet, and B. Aufray, *Appl. Phys. Lett.* 97 (1010) 223109.

- [2] P. Vogt, P. De Padova, C. Quaresima, J. A. E. Frantzeskakis, M. C. Asensio, A. Resta, B. Ealet, and G. L. Lay, *Phys. Rev. Lett.* 108 (2012) 155501.
- [3] B. Feng, Z. Ding, S. Meng, Y. Yao, X. He, P. Cheng, L. Chen, and K. Wu, *Nano Lett.* 12 (2012) 3507.
- [4] L. Meng, Y. Wang, L. Zhang, S. Du, R. Wu, L. Li, Y. Zhang, G. Li, H. Zhou, W. A. Hofer, and H. -J. Gao, *Nano. Lett.* 13 (2013) 685.
- [5] A. Fleurence, R. Friedlein, T. Ozaki, H. Kawai, Y. Wang, and Y. Yamada-Takamura, *Phys. Rev. Lett.* 108, (2012) 245501.
- [6] D. Chiappe, E. Scalise, E. Cinquanta, C. Grazianetti, B. van den Broek, M. Fanciulli, M. Houssa and A. Molle, *Adv. Mat.* 26 (2014) 2096.
- [7] L. Li, S.-Z. Lu, J. Pan, Z. Qin, Y.-Q. Wang, Y. Wang, G.-Y. Cao, S. Du and H.-J. Gao, *Adv. Mat.* 26 (2014) 4820.
- [8] L. Zhang, P. Bampoulis, A. N. Rudenko, Q. Yao, A. van Houselt, B. Poelsema, M. I. Katsnelson and H. J. W. Zandvliet, *Phys. Rev. Lett.* 116 (2016) 256804.
- [9] F. Zhu, W. -J. Chen, Y. Xu, Ch. -L. Gao, D. -D. Guan, C. Liu, D. Qian, Sh. -Ch. Zhang, J. -F. Jia, *Nat. Mater.* 14 (2015) 1020.
- [10] C.-C. Liu, W. Feng and Y. Yao, *Phys. Rev. Lett.* 107 (2011) 076802.
- [11] C.-C. Liu, H. Jiang, and Y. Yao, *Phys. Rev. B* 84, (2011) 195430.
- [12] N. D. Drummond, V. Z'olyomi and V. I. Fal'ko, *Phys. Rev. B* 85 (2012) 075423.

- [13] Y. Xu, P. Tang, Sh.-Ch. Zhang, Phys. Rev. B 92 (2015) 081112.
- [14] H. Pan, Z. Li, C.-C. Liu, G. Zhu, Z. Qiao and Y. Yao, Phys. Rev. Lett. 112 (2014) 106802.
- [15] M. Ezawa, Phys. Rev. Lett. 109 (2012) 055502.
- [16] M. Tahir and U. Schwingenschlogl, Sci. Rep. 3 (2013) 1075.
- [17] H. Zhou, Y. Cai, G. Zhang, Y. -W. Zhang, Phys. Rev. B 94 (2016) 045423.
- [18] M. Ezawa, Phys. Rev. Lett. 114 (2015) 056403.
- [19] C. J. Tabert and E. J. Nicol, Phys. Rev. Lett. 110 (2013) 197402.
- [20] M. Ezawa, Phys. Rev. Lett. 110 (2013) 026603.
- [21] X.-T. An, Y.-Y. Zhang, J.-J. Liu and S-S. Li, New J.Phys. 14 (2012) 083039.
- [22] W.-F. Tsai, C.-Y. Huang, T.-R. Chang, H. Lin, H.-T. Jeng and A. Bansil, Nat. Commun. 4 (2013) 1500.
- [23] M. Ezawa, J. Phys. Soc. Jpn. 84 (2015) 121003.
- [24] B. Soodchomshom, J. Appl. Phys. 115 (2014) 023706.
- [25] Y. Wang, Appl. Phys. Lett. 104 (2014) 032105.
- [26] N. Missault, P. Vasilopoulos, V. Vargiamidis, F. M. Peeters and B. Van Duppen, Phys. Rev. B 92, (2015) 195423.
- [27] Y. Mohammadi and B. Arghavani Nia, Superlattices and Microstructures 88 (2015) 442.

- [28] H. Min, J. E. Hill, N. A. Sinitsyn, B. R. Sahu, L. Kleinman and A. H. MacDonald, Phys. Rev. B 74 (2006) 165310.
- [29] S. Sanvito, Chem. Soc. Rev. 40 (2011) 3336.
- [30] B. Huang, D. J. Monsma and I. Appelbaum, Phys. Rev. Lett. 99 (2007) 177209.
- [31] Y. Wang, J. Zheng, Z. Ni, R. Fei, Q. Liu, R. Quhe, C. Xu, J. Zhou, Z. Gao, J. Lu, Nano 07 (2012) 1250037.
- [32] T. Gunst, T. Markussen, K. Stokbro and M. Brandbyge, Phys. Rev. B 93 (2016) 035414.
- [33] T. Yokoyama, Phys. Rev. B(R) 87 (2013) 241409.
- [34] H. Haugen, D. Huertas-Hernando, and A. Brataas, Phys. Rev. B 77, (2008) 115406.
- [35] P. Wei, S. Lee, F. Lemaitre, L. Pinel, D. Cutaia, W. Cha, F. Katmis, Y. Zhu, D. Heiman, J. Hone, J. S. Moodera, Ch.-T. Chen, Nat. Mater. 15 (2016) 711.
- [36] Zh. Wang, Ch. Tang, R. Sachs, Y. Barlas, and J. Shi, Phys. Rev. Lett. 114 (2015) 016603.
- [37] X. Zhai, S. Zhang, Y. Zhao, X. Zhang and Z. Yang, Appl. Phys. Lett. 109 (2016) 122404.
- [38] X Zhai, Sh. Wang, Y. Zhang, New. J. Phys. 19 (2017) 063007
- [39] V. P. Gusynin, S.G. Sharapov and A. A. Varlamov, Phys. Rev. B 90 (2014) 155107.
- [40] Y. H. Wang, H. Steinberg, P. Jarillo-Herrero, and N. Gedik, Science 342 (2013) 453.
- [41] E. J. Sie, J. M. McIver, Y-. H. Lee, L. Fu, J. Kong, and N. Gedik, Nature Materials 14 (2015) 290.

- [42] T. Kitagawa, T. Oka, A. Brataas, L. Fu and E. Demler, Phys. Rev. B 84 (2011) 235108.
- [43] M. Tahir and U. Schwingenschlögl, New J. Phys. 16 (2014) 115003.
- [44] Y. Mohammadi and B. Arghavani Nia, Superlattices and Microstructures 96 (2016) 259.
- [45] J. Tworzydło, B. Trauzettel, Titov, A. Rycerz and C. W. J. Beenakker, Phys. Rev. Lett. 96 (2006) 246802.
- [46] H. Bruus and K. Flensberg, Many-Body Quantum Theory in Condensed Matter Physics: An Introduction, Oxford University Press, Oxford, 2004.
- [47] M. I. Alomar, D. Sanchez, Phys. Rev. B 89 (2014) 115422.
- [48] Zh. P. Niu, Y. M. Zhang and Sh. Dong, New. J. Phys. 17 (2014) 073026.
- [49] K. S. Novoselov, A. K. Geim, S. M. Morozov, D. Jiang, Y. Zhang, S. V. Dubonos, I. V. Grigorieva, and A. A. Firosov, Science 306 (2004) 666.
- [50] C. S. Praveen, S. Piccinin and S. Fabris, Phys. Rev. B 92 (2015) 075403.

Table 1: The table presents geometrical and electrical parameters (a , λ_{so1} , λ_{so2} , v_F and γ) of silicene (Si), germanene (Ge) and stanene (Sn) taken from Ref. [11]. γ has been obtained using Eq. 43 of Ref. [11].

system	$a(\text{\AA})$	$\lambda_{so1}(meV)$	$\lambda_{so2}(meV)$	$v_F(10^5 m/s)$	$\gamma(eV)$
Silicene	3.86	3.9	0.073	5.52	1.043
Germanene	4.02	43	3.3	4.57	0.864
Stanene	4.70	29.9	34.9	4.85	0.784

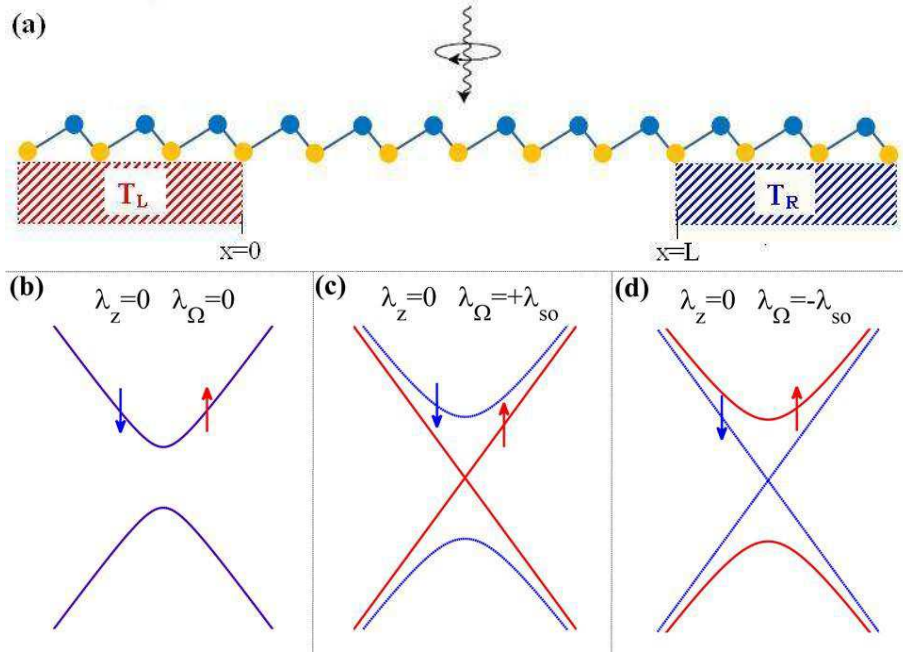


Figure 1: (a) A schematic diagram of a LBDM-based junction, whose central region is subjected to off-resonant circularly polarized light. Electronic transport is activated with a temperature gradient ($T_L - T_R$) between the two hot(L) and cold(R) electrodes. (b), (c) and (d) represent the energy spectrum of the spin-up (red curve) and spin-down (blue curve) energy bands in the central region for $\lambda_\Omega = 0$, $\lambda_\Omega = +\lambda_{so}$ and $\lambda_\Omega = -\lambda_{so}$ respectively

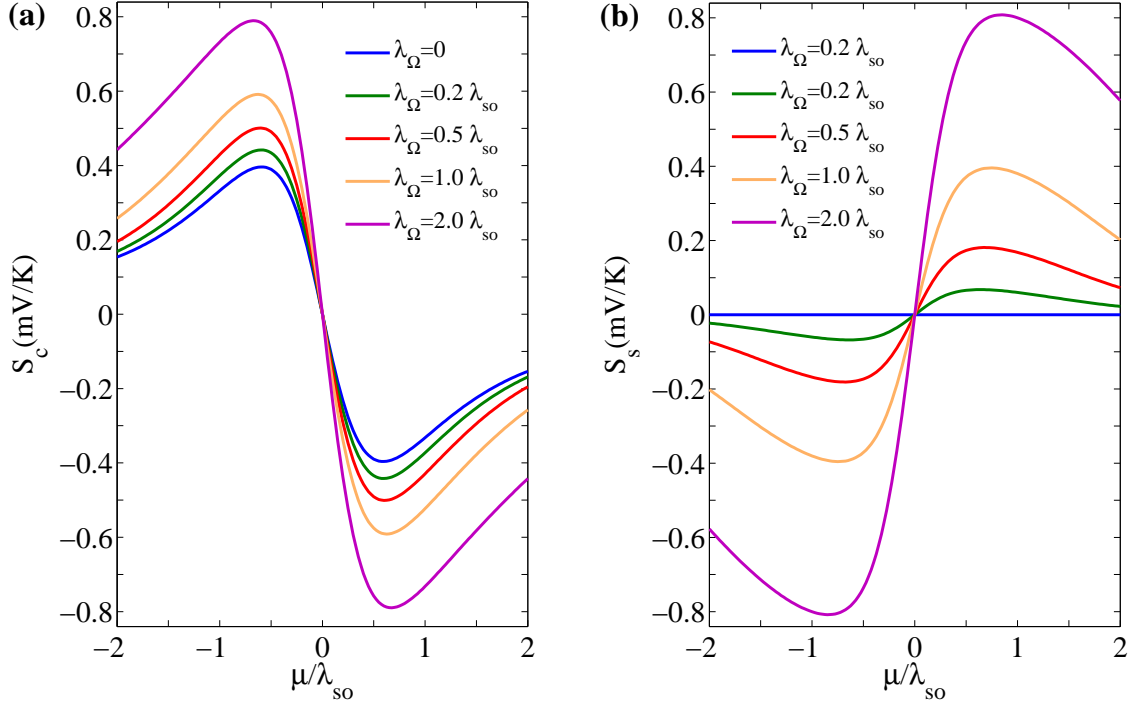


Figure 2: (a) Charge and (b) spin thermopower of an irradiated LBDM-based junction as functions of dimensionless chemical potential for different values of λ_Ω . The other parameters are $\lambda_z = 0$, $T = 0.4\lambda_{so}$ and $L = 130a$.

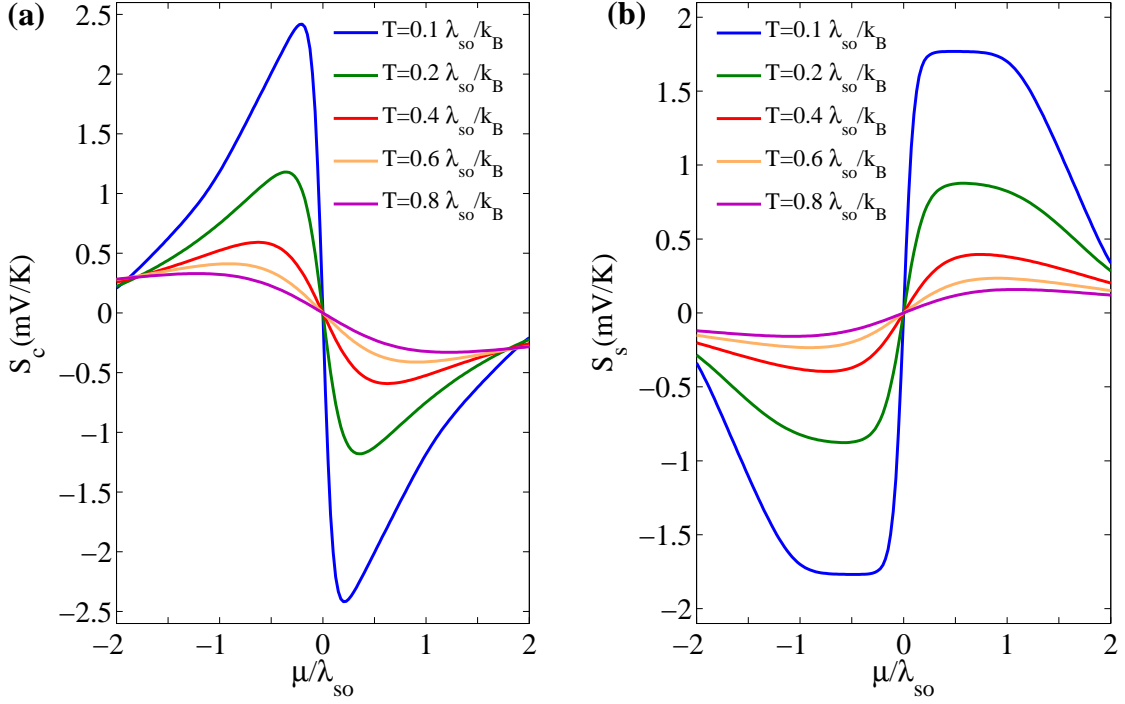


Figure 3: (a) Charge and (b) spin thermopower of an irradiated LBDM-based junction as functions of dimensionless chemical potential for different values the junction temperature.

The other parameters are $\lambda_z = 0$, $\lambda_\Omega = \lambda_{so}$ and $L = 130a$.

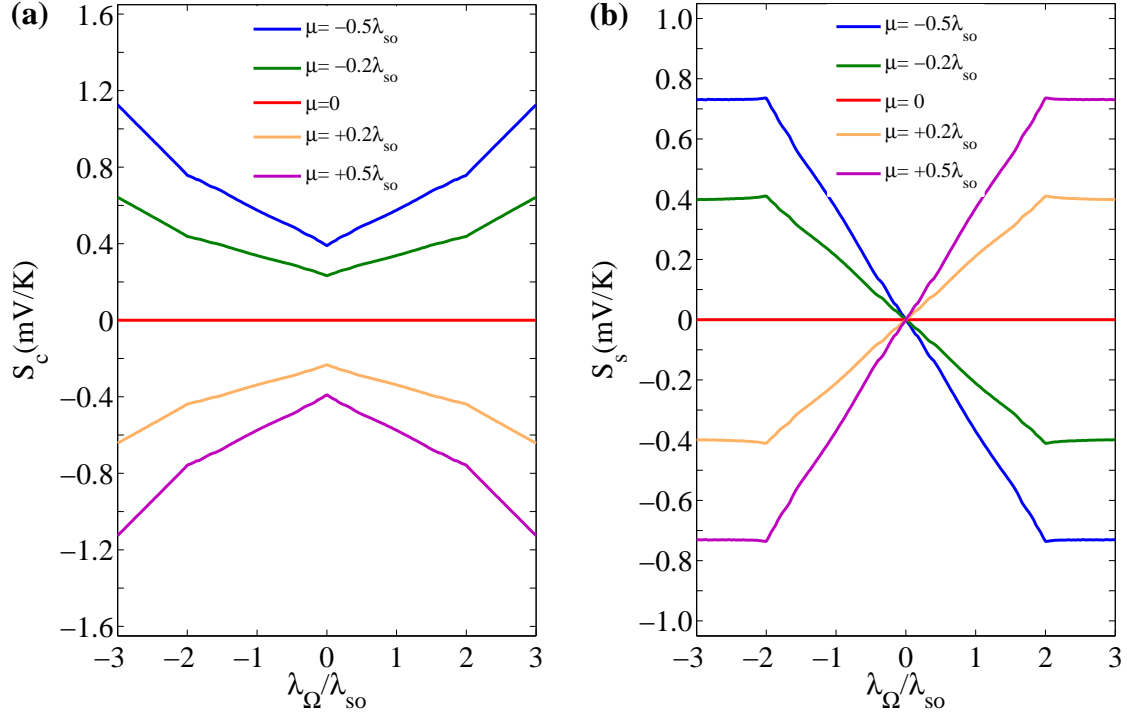


Figure 4: (a) Charge and (b) spin thermopower of an irradiated LBDM-based junction as functions of $\lambda_\Omega/\lambda_{so}$ for different values of the chemical potential. The other parameters are $\lambda_z = 0$, $T = 0.4\lambda_{so}$ and $L = 130a$.

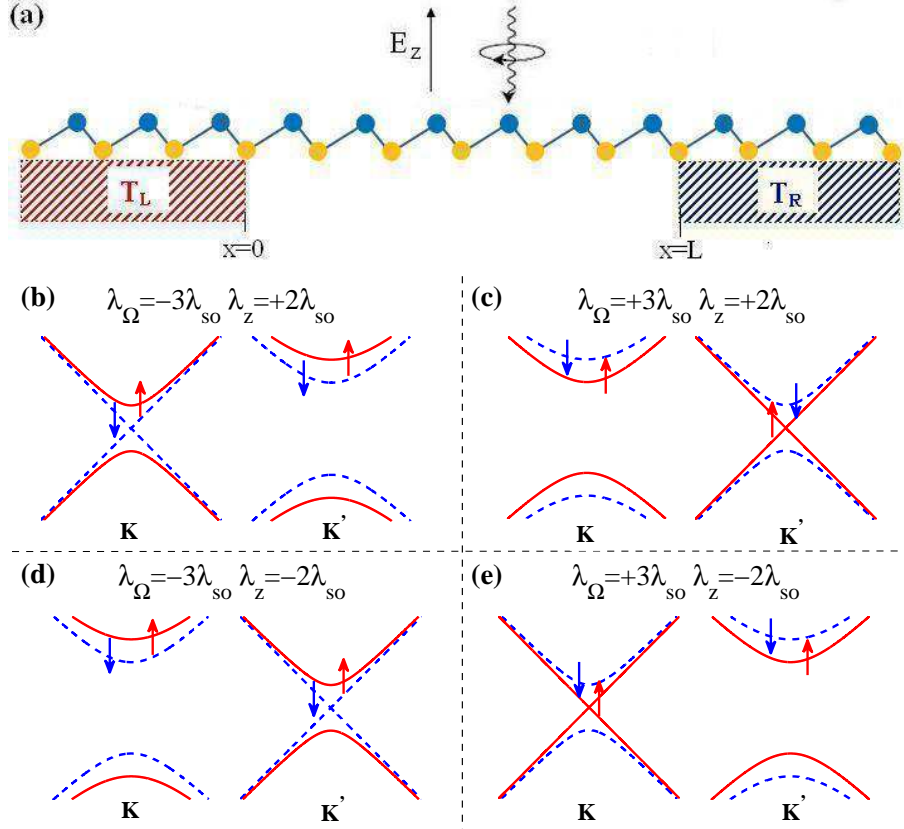


Figure 5: (a) A schematic diagram of a LBDM-based junction, whose central region is subjected to a perpendicular electric field and off-resonant circularly polarized light simultaneously. (b), (c), (d) and (e) represent the energy spectrum of the central region for the spin-up (red curve) and spin-down (blue curve) electrons at both Dirac points for different values of λ_Ω and λ_z .

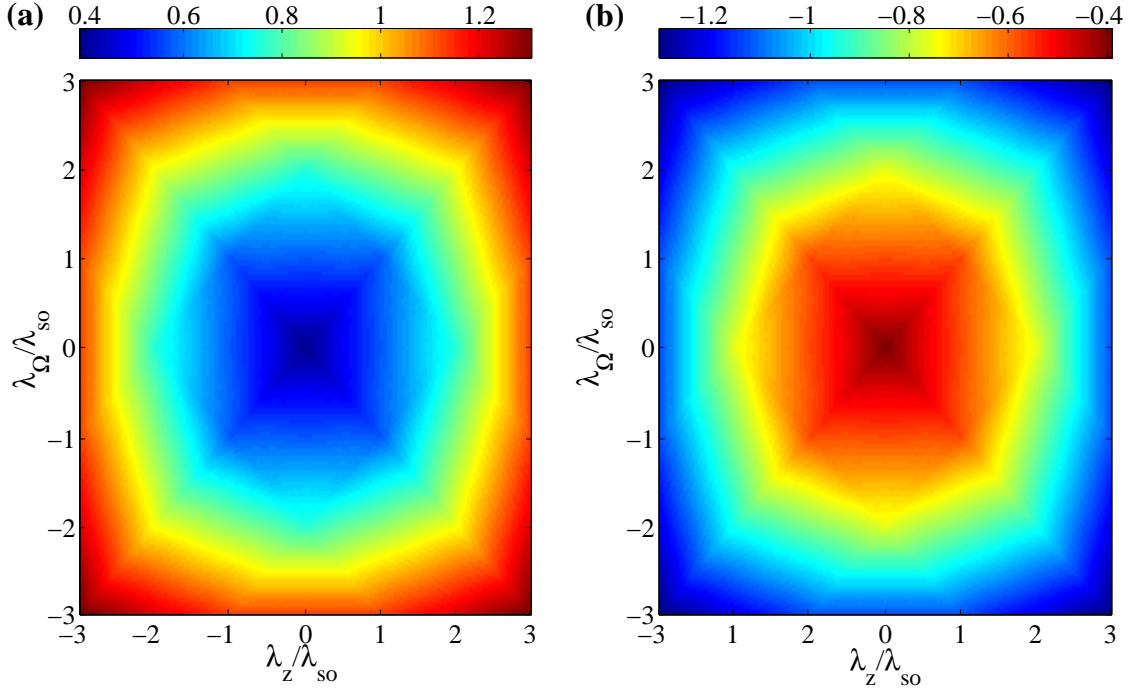


Figure 6: Charge thermopower of an irradiated LBDM-based junction as functions of $\lambda_\Omega/\lambda_{so}$ and λ_z/λ_{so} for (a) $\mu = -0.5\lambda_{so}$ and (b) $\mu = +0.5\lambda_{so}$. The other parameters are $T = 0.4\lambda_{so}/k_B$ and $L = 130a$.

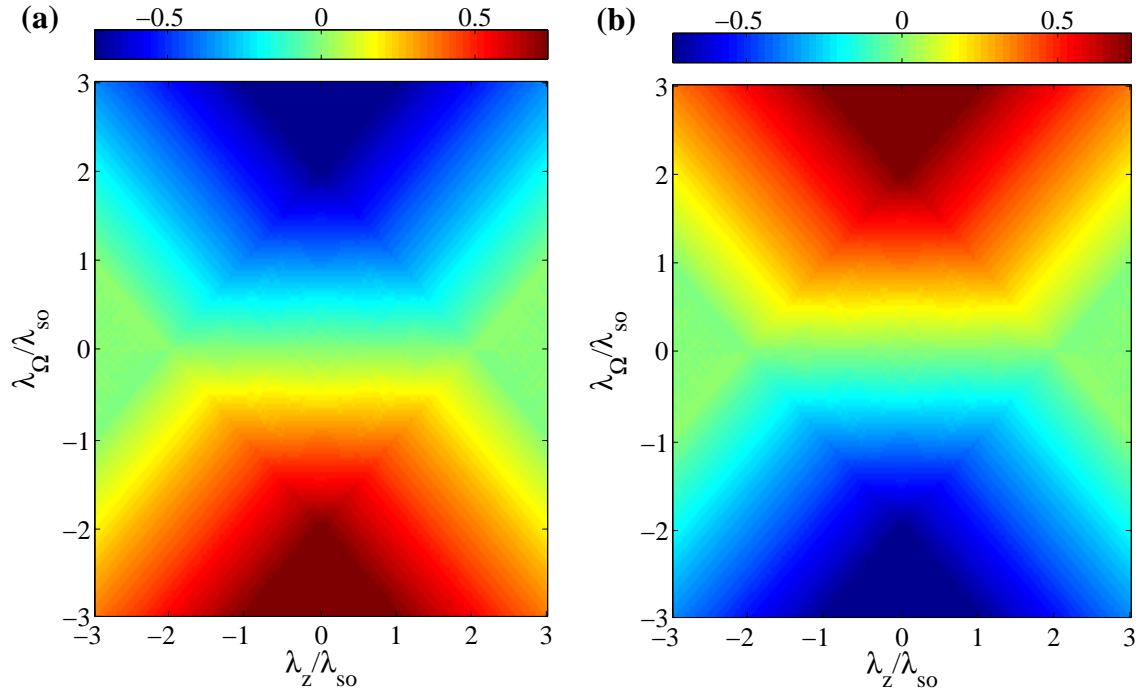


Figure 7: Spin thermopower of an irradiated LBDM-based junction as functions of $\lambda_\Omega/\lambda_{so}$ and λ_z/λ_{so} for (a) $\mu = -0.5\lambda_{so}$ and (b) $\mu = +0.5\lambda_{so}$. The other parameters are $T = 0.4\lambda_{so}/k_B$ and $L = 130a$.

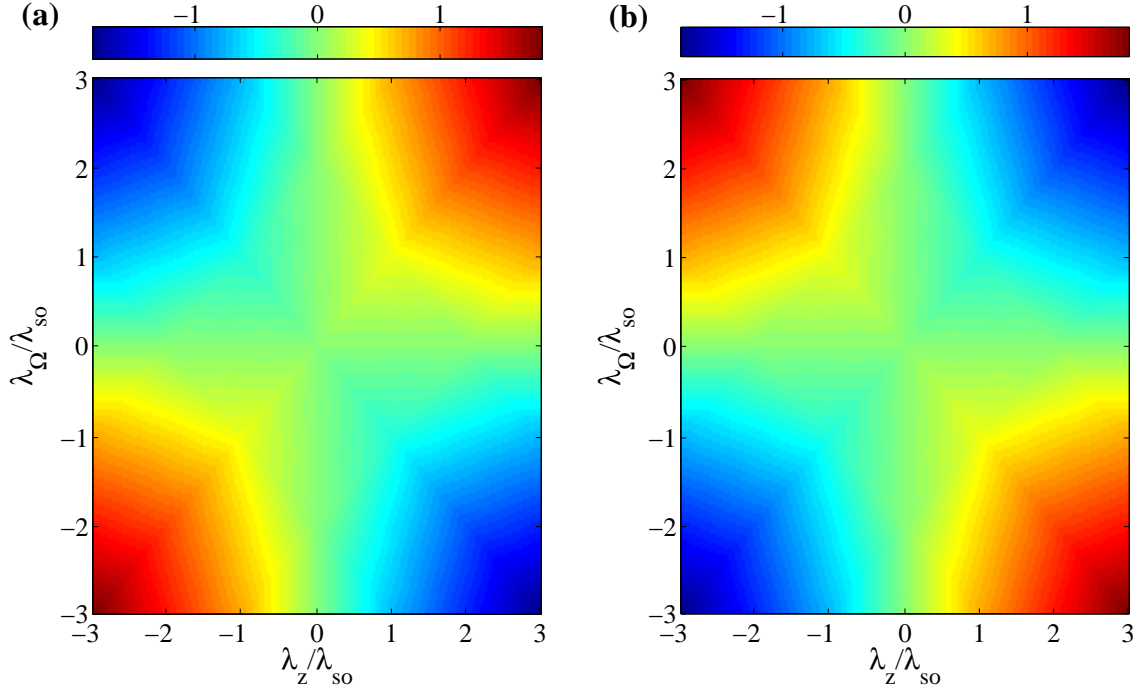


Figure 8: Valley thermopower of an irradiated LBDM-based junction as functions of $\lambda_\Omega/\lambda_{so}$ and λ_z/λ_{so} for (a) $\mu = -0.5\lambda_{so}$ and (b) $\mu = +0.5\lambda_{so}$. The other parameters are $T = 0.4\lambda_{so}/k_B$ and $L = 130a$.